
Scalable Neural Network Verification against Geometric Perturbations via Hölder Optimisation

Anonymous Author(s)

Affiliation

Address

email

Abstract

1 Neural Network (NN) verification methods provide local robustness guarantees for
2 a NN in the dense perturbation space of an input point. A key challenge in this area
3 lies in the scalability of the resulting problem, leading to large models of interest
4 in applications not being addressable by the methods. In this paper we introduce
5 HOVER, a method for the verification of NNs against geometric perturbations, that
6 uniquely employs a Hilbert space-filling construction to reduce multidimensional
7 problems to single-dimensional ones. The underlying Hölder optimisation, which
8 also iteratively refines the estimation for the Hölder constant for constructing the
9 lower bound, theoretically it may converge to a local minimum, thereby resulting
10 in a robustness result being incorrect. However, we show experimentally that this
11 risk can be contained in practice by appropriately devised heuristics in the global
12 optimisation setup. Indeed, unlike recently reported errors from theoretically sound
13 implementations, we found no incorrect result by running the technique on a large
14 set of benchmarks from SoundnessBench and VNN-COMP. To validate the scal-
15 ability of the approach, we report on extensive experiments on large NNs ranging
16 from Resnet34 to Resnet152 and ViTs. These demonstrate the SoA performance of
17 the approach in evaluating with high reliability the local robustness of large NNs
18 against geometric perturbations on the ImageNet dataset. Beyond image tasks, we
19 show that the method’s scalability enables for the first time robustness assessments
20 for large-scale 3D-NNs in video classification tasks against geometric perturbations
21 for long-sequence input frames on Kinetics/UCF101 datasets.

22

1 Introduction

23 As well known, Neural Networks (NNs) are inherently vulnerable to adversarial perturbations [1],
24 *i.e.*, their output is often susceptible to fragilities, or attacks, in the neighbourhood of correctly
25 processed inputs. In the context of machine vision models, input perturbations generating such
26 fragilities can take various forms including noise, geometric changes, illumination variations, and
27 beyond. Evaluating the robustness of a model, *i.e.*, the resistance to such vulnerabilities, is particularly
28 important in safety-critical applications.

29 The area of robustness verification [2] consists of methods providing formal guarantees that a model
30 is locally robust in regions of the input space defined by a test point and a particular perturbation. A
31 well-known difficulty of these methods is their scalability: the problem is theoretically NP-hard [3]
32 and present SoA methods do not scale to neither large models used in applications, nor large inputs,
33 nor large perturbations [4], thereby hindering the application of these methods in applications.

34 With the exceptions discussed in Related Work (Section 5), methods for the verification of local
35 robustness are sound, *i.e.*, if the method reports that the model is locally robust in a region, that is
36 theoretically guaranteed to be the case. While this result provides theoretical comfort, arguably it

37 is less significant in practice. Firstly, the actual correctness of a specific verification query may be
38 hindered by floating point precision errors at system level as well as other issues [5], as recently
39 evidenced in [6], thereby rendering such guarantees less significant in practice. Secondly, overall
40 considerations on the robustness of a model are derived by analysing thousands or more input points
41 and perturbations of various sizes. It is the aggregation of these results, not a single query, that
42 enables the analysis of a model’s robustness as well as the comparison between models.

43 Therefore, as long as errors can be well-contained in practice, the theoretical soundness of a method
44 appears less essential compared to whether or not the method can scale to models in use in applications.
45 Indeed, adversarial testing is routinely used in applications to evaluate the robustness of large
46 models [7, 8]. Yet, adversarial testing is well-known to fail to identify fragilities in a very large
47 number of cases, potentially instilling a false sense of robustness in the developer.

48 In this paper, we exploit the observations above to introduce HOVER, a method based on Hölder
49 optimisation that exploits dimensionality reduction to scale to large models with hundreds of mil-
50 lions of parameters. HOVER is inspired by recent advanced developments in the area of global
51 optimisation [9–11]. As such, in theory, in line with many global optimisation methods [12] for
52 NN verification, its convergence to the global minimum can be assured only if some appropriate
53 optimisation parameters are chosen. We return to this aspect in Section 5, where we observe that
54 most existing global optimisation-based approaches also have this property.

55 In practice, we demonstrate that the optimisation problem can be appropriately formulated, resulting
56 in no incorrect results on the large-scale benchmarks that we study, including SoundnessBench, and
57 outperforming in practice all current SoA and theoretically sound methods.

58 In summary, the paper contributions are as follows:

- 59 • We propose HOVER, a global optimisation method for the verification of NNs based on
60 space-filling dimensionality reduction and Hölder optimisation. We provide theoretical
61 conditions for convergence, hence soundness. We illustrate that such conditions are difficult
62 to ascertain in practice but that, experimentally, the potential of error in a single query is
63 well contained. Indeed, no errors were produced following extensive evaluation including
64 SoundnessBench [6].
- 65 • We use HOVER to verify the local robustness of models up to 300M tuneable parame-
66 ters, including ResNet152 and Vision Transformers for image classification tasks, against
67 geometric properties (rotation, scaling, and translation) on the large-scale ImageNet dataset.
- 68 • We use HOVER to verify for the first time the geometric robustness of 3D ResNet models in
69 video classification tasks for streams of $32 \times 3 \times 256 \times 256$ inputs.

70 We believe these results enable a robustness analysis of large models used in applications that could
71 not be undertaken before other than via adversarial search, which has a much lower confidence rate.

72 The rest of the paper is organised as follows. In Section 2 we present key notions of use throughout.
73 We present HOVER in Section 3 where we give the technical details of the algorithm. In Section 4,
74 we evaluate HOVER on large NNs for image classification and video classification; we also evaluate
75 the correctness of the implementation empirically on SoundnessBench and additional benchmarks
76 from VNN-COMP [4]. Section 5 discusses related work. We conclude in Section 6.

77 2 Preliminaries

78 This section outlines the background concepts and notation that facilitate the exposition of the
79 verification method presented in the next section.

80 **Hölder/Lipschitz constant.** A function $f : \mathbb{R}^N \rightarrow \mathbb{R}$ is said to be Hölder continuous with exponent
81 $\alpha \in (0, 1]$ if there exists a smallest constant $H \geq 0$, called the Hölder constant, such that for all
82 $x, x' \in [a, b]$, the following inequality holds: $|f(x) - f(x')| \leq H|x - x'|^\alpha$. Lipschitz continuity [13]
83 is a special case of Hölder continuity when $\alpha = 1$, in which case H becomes the Lipschitz constant
84 L . These constants represent the highest rate at which the function can change in the interval.

85 **Hilbert space-filling curve.** A space-filling curve [14] is a function $h : \mathbb{R} \rightarrow \mathbb{R}^N$ that maps the unit
86 interval $x \in [0, 1]$ onto a multidimensional hypercube $D = \{\boldsymbol{\theta} \in [a, b]^N\} \subset \mathbb{R}^N$:

$$\{h(x) : 0 \leq x \leq 1\} = \{\boldsymbol{\theta} \in \mathbb{R}^N : a \leq \theta_i \leq b, i \in N\}. \quad (1)$$

87 The function h is surjective; so for every point in the hypercube, there exists at least one point in the
 88 interval which maps onto it.

89 The first examples of space-filling curves date back to Peano [14]; the one we adopt here is due
 90 to Hilbert [15]. Their definition is given in the limit of infinitely many refinements of recursive
 91 constructions. Each recursive step discretises the space at a fixed resolution determined by a parameter
 92 m , thereby producing an m -approximation of the space. Specifically, the hypercube D is subdivided
 93 into $2^{N \times m}$ smaller hypercubes with 2^m subdivisions along each dimension. The Hilbert curve
 94 for an m -approximation, denoted $h_{N,m}$, traverses these unit hypercubes in a continuous manner,
 95 thus preserving spatial locality. As $m \rightarrow \infty$, the approximation converges to the true space-filling
 96 Hilbert curve, which fully covers the entire hypercube in the limit. An example of Hilbert curves
 97 $h_{N=3,m=3}(\cdot)$ can be seen on the left of Figure 1.

98 A property of Hilbert curves is that the multi-dimensional minimisation problem of a Lipschitz
 99 continuous function $f : \mathbb{R}^N \rightarrow \mathbb{R}^c$ ($N, c \in \mathbb{R}$) can be accurately reduced to the one-dimensional
 100 problem along the m -approximation of the Hilbert curve $h_{N,m}$ [16]:

$$\min_{\theta \in \mathbb{R}^N} f(\theta) = \min_{x \in [0,1]} f(h(x)) \approx \min_{x \in [0,1]} f(h_{N,m}(x)) = \min \tilde{f}(x); \quad (2)$$

101 where for brevity $\tilde{f}(x)$ denotes $f(h_{N,m}(x))$. Further, $\tilde{f}(x)$ is Hölder continuous with exponent
 102 $\alpha = 1/N$:

$$\forall x, x' \in [0, 1]: |\tilde{f}(x) - \tilde{f}(x')| \leq H(|x - x'|)^{\frac{1}{N}}, \quad (3)$$

103 where $H = 2L\sqrt{N+3}$ is the Hölder constant and L is the Lipschitz constant of the original f .

104 **Neural Networks with Lipschitz continuity.** We consider Lipschitz continuous neural networks
 105 (NNs) $g : \mathbb{R}^N \rightarrow \mathbb{R}^c$. NNs comprising convolutional, fully connected, and contrast normalisation
 106 layers with ReLU activation functions are Lipschitz continuous [17]. Further, softmax layers, as well
 107 as sigmoid and hyperbolic tangent activation functions, also satisfy Lipschitz continuity [18]. We
 108 here focus on classification tasks where each input $x \in \mathbb{R}^N$ is assigned to the class \hat{y} among a set of
 109 classes $\{1, \dots, c\}$ determined by the largest NN output, *i.e.*, $\hat{y} = \arg \max_{j=1, \dots, c} g(x)_j$.

110 **Local robustness verification.** Given a NN $g : \mathbb{R}^N \rightarrow \mathbb{R}^c$, an input x to g , and a perturbation space
 111 $\Omega(x)$ of x , the robustness verification problem establishes whether the class prediction of the network
 112 is consistent within the perturbation space. In other words, the problem is to determine whether:

$$\forall x' \in \Omega(x): \arg \max_i g(x)_i = \arg \max_i g(x')_i. \quad (4)$$

113 By taking $f(g, x, x') = g(x')_y - \max_{i \neq y} g(x')_i$, where $y = \arg \max_i g(x)_i$, this is equivalent to
 114 establishing whether:

$$\forall x' \in \Omega(x): f(g, x, x') > 0. \quad (5)$$

115 A NN g is said to be certifiably robust on input x with respect to the perturbation space $\Omega(x)$ if Eq. (5)
 116 holds. Any violation of this property, *i.e.*, $\exists x' \in \Omega(x): f(g, x, x') < 0$, indicates the presence of a
 117 counterexample. A common perturbation space is the one generated by ℓ_p norms around x , defined
 118 as $\Omega(x) = \{x': \|x - x'\|_p \leq \epsilon\}$ for a perturbation budget $\epsilon \in \mathbb{R}$.

119 **Local geometric robustness.** A perturbation space that is of particular interest in computer vision
 120 is defined in terms of geometric perturbations on the input, such as rotation, translation, scaling or
 121 combinations thereof [19]. A geometric perturbation is a 2D affine transformation A_θ that provides
 122 a mapping between source coordinates (x^s, y^s) of the input and target coordinates (x^t, y^t) of the
 123 transformed input:

$$\begin{bmatrix} x^s \\ y^s \\ 1 \end{bmatrix} = A_\theta \begin{bmatrix} x^t \\ y^t \\ 1 \end{bmatrix} = \begin{bmatrix} \lambda \cos \gamma & -\sin \gamma & t_{\text{hor}} \\ \sin \gamma & \lambda \cos \gamma & t_{\text{ver}} \end{bmatrix} \begin{bmatrix} x^t \\ y^t \\ 1 \end{bmatrix}, \quad (6)$$

124 where $\theta = [\gamma, \lambda, t^{\text{hor}}, t^{\text{ver}}]$ are the transformation parameters, with γ representing the rotation angle,
 125 λ denoting the scaling factor, and $t^{\text{hor}}, t^{\text{ver}}$ controlling the horizontal and vertical translation. Each
 126 pixel value V_{x^s, y^s} in the transformed image can be computed by calculating the pre-image of the pixel
 127 under A_θ and interpolating the (possibly non-integer) resulting coordinates using any interpolation
 128 scheme. We here adopt Spatial Transformation Networks [20] with bilinear interpolation to determine

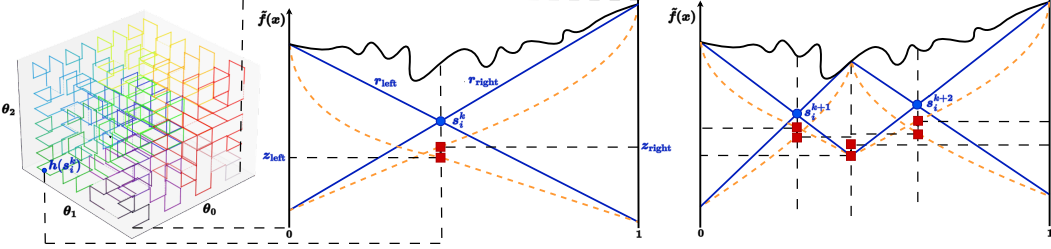


Figure 1: From left to right: Hilbert curve mapping; k -th iteration of HOVER’s optimisation; The subsequent iterations of HOVER’s optimisation.

129 these values: $V_{x^t, y^t} = \sum_n^H \sum_m^W U_{nm} \max(0, 1 - |x^s - m|) \max(0, 1 - |y^s - n|)$, where U_{hw} is
130 the value of the pixel with coordinates (n, m) .

131 Given interval constraints $\Theta \subset \mathbb{R}^4$, the geometric perturbation space $\Omega(\mathbf{x}) = \{V(\mathbf{x}, \boldsymbol{\theta}) \mid \boldsymbol{\theta} \in \Theta\}$
132 for an input \mathbf{x} is the set of all transformed inputs for each $\boldsymbol{\theta} \in \Theta$, where each transformed input
133 $V(\mathbf{x}, \boldsymbol{\theta})$ is obtained by determining $V_{x,y}$ for each pixel (x, y) of the input. Establishing the local
134 robustness of NNs with respect to this space can be used to assess their robustness to geometric
135 distortion effects, such as tilted camera orientation (rotation), positional shifts (translation), and zoom
136 variations (scaling) [21].

137 The space has two important properties that enable the derivation and efficacy of the verification
138 procedure introduced in the next section. First, prepending geometric transformation modules to
139 Lipschitz continuous NNs preserves Lipschitz continuity, as proved in [22]. Second, the perturbation
140 dimensionality of these modules is very low (the number of parameters) when compared to the input
141 dimensionality of norm-based perturbation modules (the number of pixels). We will exploit this to
142 provide an effective reduction to one dimension in a method that enables for the first time scalable
143 global optimisation-based verification for more than one input dimensions.

144 We hereafter consider the local geometric robustness problem $\forall \boldsymbol{\theta} \in \Theta : f(g', \mathbf{x}, V(\mathbf{x}, \boldsymbol{\theta})) > 0$,
145 where g' denotes a NN prepended with a geometric module on input \mathbf{x} [19]. Since g' and \mathbf{x} are fixed,
146 we briefly denote the problem by $\forall \boldsymbol{\theta} \in \Theta : f(\boldsymbol{\theta}) > 0$.

147 3 Hölder-based Global Optimisation for Neural Network Verification

148 This section puts forward HOVER, a Hölder-based optimisation method for solving the robustness
149 verification problem defined in the previous section. The method aims to find a solution to the
150 optimisation problem $\min f(\boldsymbol{\theta})$ s.t. $\boldsymbol{\theta} \in \Theta$, where Θ is an N -dimensional hyperrectangle encoding
151 the perturbation space around an input. If the solution to the problem is greater than zero, then the
152 verification problem can be answered positively. To enable the utilisation of scalable 1D methods,
153 HOVER first transforms the multivariate function of the optimisation problem into a univariate
154 equivalent using the Hilbert space filling-curve. Some optimisation methods for the resulting univari-
155 ate problem require knowledge of the Hölder constant [23], while some others do not [11].
156 Following the intractability of the accurate estimate of the constant [9], we here adapt a method from
157 the latter category that relies on adaptive estimations of the constant throughout the optimisation
158 process [9, 10, 18]. As we discuss in more detail below, while the method does not theoretically
159 guarantee the identification of the global minimisers of the optimisation objective, it scores higher on
160 soundness than leading, theoretically sound verification frameworks, while exhibiting significantly
161 higher scalability. This is enabled by common optimisation practices that we employ and this section
162 outlines.

163 In the following, we provide a technical exposition of HOVER. To ease its presentation, and without
164 loss of generality, we assume that the input domain Θ has been normalised to the hypercube $[0, 1]^N$.
165 We begin with a short technical overview.

166 **Overview.** Figure 1 illustrates the first two iterations of HOVER. Having transformed the multi-
167 variate objective function into a univariate one, the algorithm iteratively operates on increasingly
168 tighter intervals of the (one-dimensional) input range. For each interval, it computes a low-bounding

169 piecewise function (the orange/dashed lines in the figure) using an estimation of the Hölder constant
 170 for that interval. Based on this low-bounding function, it then computes a lower bound for the
 171 interval (the minimum between z_{left} and z_{right} in the figure). At each iteration, the algorithm chooses
 172 the interval with the lowest bound to split into tighter intervals at the point where the estimated
 173 lower bound is observed. Lower-bounding functions for the new sub-intervals are then computed to
 174 facilitate the next iteration. The algorithm terminates when an optimisation budget ϵ is reached that
 175 reflects the minimum length of the selected interval. Below, we discuss this procedure in detail.

176 **Initialisation.** HOVER is initialised by: (i) transforming the multi-dimensional optimisation problem
 177 $\min f(\theta)$ s.t. $\theta \in [0, 1]^N$ to the one-dimensional problem $\min \tilde{f}(x)$ s.t. $x \in [0, 1]$ using the Hilbert
 178 space-filling curve, (ii) setting $\mathcal{I} = \{[0, 1]\}$ to be the set of initial intervals, and (iii) letting $\mathcal{O} = \{\}$
 179 to be the set of already considered intervals. Then, for each iteration $k \geq 1$, HOVER executes the
 180 following steps.

181 **Step 1 (Adaptive estimation of the Hölder constant).** For each interval $i \in \mathcal{I}$, with $i = [a, b]$,
 182 HOVER computes a *local* Hölder constant $H_i = \frac{|\tilde{f}(b) - \tilde{f}(a)|}{|a - b|^{\frac{1}{N}}}$, and a *global* Hölder constant $h_k =$
 183 $\max\{H_i \mid i \in \mathcal{I}\}$. Based on these constants, it derives its (adaptive) estimation of the Hölder constant
 184 for interval i as $\hat{H}_i = r \cdot \max\{\lambda, \gamma, \xi\}$, where:

- 185 • $\lambda = \max\{H_j \mid j = i \text{ or } j \text{ is adjacent to } i\}$ is the local component of the estimation that
 186 reflects the maximum constant between the local constants of interval i and its adjacent
 187 intervals (*i.e.*, intervals that have a common bound);
- 188 • $\gamma = h_k \frac{|a - b|}{X_{\max}}$ is the global component of the estimation, where $X_{\max} =$
 189 $\max\{(b' - a')^{\frac{1}{N}} \mid [a', b'] \in \mathcal{I}\}$ is the widest interval;
- 190 • ξ is a small value that prevents \hat{H}_i from becoming 0, accounting for $\tilde{f}(x)$ varying over $[0, 1]$;
- 191 • $r > 1$ is the reliability parameter of the algorithm.

192 Intuitively, the adaptive estimation \hat{H}_i is dominated by the global component whenever an interval is
 193 large (and thus the local estimates are not reliable), and by the local component whenever an interval
 194 is small (and thus the local estimates are more accurate). As discussed in more detail below, the
 195 reliability parameter r mitigates potential underestimations of the constant.

196 **Step 2 (Estimation of the lower bounds of the intervals).** For each interval $i \in \mathcal{I}$, with $i = [a, b]$,
 197 the algorithm computes the point

$$s_i = \frac{b + a}{2} - \frac{\tilde{f}(b) - \tilde{f}(a)}{2\hat{H}_i(b - a)^{\frac{1-N}{N}}}. \quad (7)$$

198 This point is the intersection of the lines $r_{\text{left}}(x)$ and $r_{\text{right}}(x)$ (see the blue/solid lines in Figure 1),
 199 which are defined as

$$\begin{aligned} r_{\text{left}}(x) &= -\hat{H}_i(b - a)^{\frac{1-N}{N}}x + \hat{H}_i(b - a)^{\frac{1-N}{N}}a + \tilde{f}(a), \\ r_{\text{right}}(x) &= \hat{H}_i(b - a)^{\frac{1-N}{N}}x - \hat{H}_i(b - a)^{\frac{1-N}{N}}b + \tilde{f}(b). \end{aligned} \quad (8)$$

200 These lines relax the piecewise lower bounding functions of \tilde{f} within the interval (the orange/dashed
 201 lines in the figure); we refer to [9] for a formal description of the functions using the estimated Hölder
 202 constant. The lower bound l_i of the interval is then estimated as $l_i = \min(z_{\text{left}}, z_{\text{right}})$, where

$$z_{\text{left}} = \tilde{f}(a) - \hat{H}_i(s_i - a)^{1/N}, \quad z_{\text{right}} = \tilde{f}(b) - \hat{H}_i(b - s_i)^{1/N}. \quad (9)$$

203 The bound l_i corresponds to the minimum value of the lower bounding functions evaluated at the s_i .

204 **Step 3 (Convergence and refinement).** HOVER selects the interval $i \in \mathcal{I}$ with the minimum lower
 205 bound estimate l_i . Then,

- 206 • If the length of the interval $i = [a, b]$ is smaller than the optimisation budget, *i.e.*, $|b - a| \leq \epsilon$,
 207 it executes to **Step 4** and terminates;
- 208 • Otherwise, it splits the selected interval with respect to $s_i = [a', b']$, and updates $\mathcal{I} \leftarrow$
 209 $\mathcal{I} \setminus \{i\} \cup \{[a, a'], [a', b']\}$, $\mathcal{O} \leftarrow \mathcal{O} \cup \{i\}$. It then repeats from **Step 1**.

210 **Step 4 (Calibration and output).** HOVER computes an estimation of the minimum of the function
 211 as $\tilde{f}_m = \min \left\{ \tilde{f}(a), \tilde{f}(b) \mid [a, b] \in \mathcal{I} \right\}$, and an estimation of the lower bound of the function as

212 $l_m = \min \{l_j \mid j \in \mathcal{I} \cup \mathcal{O}\}$. l_m is then calibrated as $l_m \leftarrow l_m - \eta$, where $\eta = L \cdot 2^{-(m+1)}\sqrt{N} +$
 213 $H \cdot (\epsilon/2)^{1/N}$, L and H being the latest estimates of the global Lipschitz and Hölder constants, and m
 214 is the resolution of the Hilbert approximation. The calibration, which is theoretically analysed below,
 215 accounts for (i) approximation errors in the dimensionality reduction along the Hilbert curve, and (ii)
 216 the constrained nature of the optimisation budget ϵ with which the algorithm operates. Following the
 217 calibration, HOVER produces its output as follows:

- 218 • If $l_m > 0$, then it returns *robust*, i.e., a positive answer to the robustness of the underlying
 219 network.
- 220 • If $\tilde{f}_m < 0$, then it returns *non-robust*, along with a counterexample $h_{N,m}(x)$ corresponding
 221 to the value for which $\tilde{f}(x) = \tilde{f}_m$.

222 We now proceed to analyse the algorithm's soundness and examine practical methods for sustaining
 223 high reliability and computational efficiency. We begin by showing that a calibrated (as per **Step 4**)
 224 lower bound for the reduced one-dimensional space translates to a lower bound for the original
 225 N -dimensional space.

226 **Theorem 1.** *Let l_h^* be a lower bound of the one-dimensional problem $\min \tilde{f}(x)$ s.t. $x \in [0, 1]$ over
 227 the Hilbert space-filling curve. Then we have that*

$$l_h^* - L \cdot 2^{-(m+1)}\sqrt{N} - H \cdot (\epsilon/2)^{1/N} \leq l^*, \quad (10)$$

228 where l^* is the optimal solution of the multi-dimensional problem $\min f(\boldsymbol{\theta})$ s.t. $\boldsymbol{\theta} \in [0, 1]^N$.

229 *Proof.* The proof is included in the Appendix. □

230 Note that the first calibration term results from the approximation of the Hilbert curve reduction, while
 231 the second is a consequence of the limited optimisation budget. When the resolution of the Hilbert
 232 approximation is high enough, e.g., $m = 50$ in our experiments, the magnitude of the former term is
 233 negligible. Differently, the magnitude of the latter term grows with the number of dimensions, thus
 234 hindering the efficacy of HOVER to high-dimensional input domains.

235 Next, we show that given a sufficiently large value for the reliability parameter r , HOVER
 236 implements a sound verification procedure.

237 **Theorem 2.** *There exists r^* s.t. for all $r > r^*$, HOVER outputs robust iff $\forall \boldsymbol{\theta} \in [0, 1]^N : f(\boldsymbol{\theta}) > 0$.*

238 *Proof.* The result follows immediately from Theorem 1 and Theorem 3.8 in [9]. □

239 Note that Theorem 2 does not provide a constructive way of determining r^* ; we conjecture that
 240 such a procedure may have high complexity. Consequently, in practice, the Hölder constant can
 241 be underestimated at any iteration and interval, which may impact the localisation of the global
 242 minimisers and the convergence speed. Note that without knowing the true Lipschitz/Hölder constant,
 243 this also applies to existing global optimisation-based verification methods [18, 24], and overlooking
 244 it may lead to potentially unsound results, even if their algorithm converges, it could be a local
 245 minimum rather than the global one. In the light of this, we below discuss operational enhancements
 246 that remedy both potential pitfalls.

247 **Practical enhancements.** To ensure high reliability, following convergence (i.e., when the optimisation
 248 budget is reached), HOVER iteratively increases the value of the reliability parameter r
 249 until either (i) a different interval is selected at **Step 3**, or (ii) a time limit (given as a parameter) is
 250 reached. Intuitively, if the algorithm converges to a local minimum following an underestimation
 251 of the Hölder constant, the iterative adjustment of the reliability parameter will eventually trigger
 252 an escape from said minimum. To further enable high practical efficacy, HOVER implements two
 253 strategies. First, it employs a heuristic whereby it dynamically adapts the Hölder constant based on
 254 both local and global information as detailed in **Step 1**. Second, for every iteration, following the
 255 selection of an interval $i = [a, b]$ and division thereof as per split point s_i at **Step 3**, it re-estimates
 256 the lower bound of an interval j at the next iteration only if one of the following conditions hold: (i)
 257 j is adjacent or contained in i ; (ii) the length of i is equal to X_{\max} ; (iii) the local Hölder constant
 258 for the subintervals of i is greater than the global Hölder constant h_k . These express the necessary
 259 conditions for triggering a change in the estimation of the lower bound l_j of each interval j (as per

Table 1: Evaluation results on 500 images from ImageNet against the perturbation combination of rotation, translation and scaling. Baselines performance is adopted from [22].

Perturbation	Model	Clean	NN	Adversarial Accuracy (%)		Certified Accuracy (%)	
		Acc	Params	GeoRobust	HOVER	GeoRobust	HOVER
R(20°) + T(10%) + S(10%)	Inception V3	73.6	24M	28.2	24.4	24.2	23.8
	ResNet34	72.0	22M	-	27.4	-	25.8
	ResNet50	78.4	26M	54.0	42.6	31.1	40.6
	ResNet101	80.0	45M	54.2	49.4	48.2	48.0
	ResNet152	79.4	60M	53.8	49.0	46.2	48.4
	Mixer	72.2	60M	27.2	24.8	23.4	24.2
	Gmlp	78.0	19M	40.8	37.6	36.8	34.2
	Swin	80.2	88M	34.6	22.2	13.2	10.0
	Large Vit _{16×16}	83.4	300M	49.2	42.2	40.2	34.8

260 the definition of the adaptive estimation of the Hölder constant \hat{H}_j in **Step 1**). Taken together these
 261 further contribute towards achieving high efficiency and a high degree of correctly computed results.

262 4 Experimental Evaluation

263 **Experimental Setup.** Our experiments were conducted on a machine equipped with an Intel i7-
 264 12700K CPU with 78GB RAM running kernel 5.15 and an RTX 3090 Ti GPU with 24GB of graphics
 265 memory. All the code is written using PyTorch, and the Hilbert space-filling curve is implemented
 266 with the hilbertcurve library [25]. Our experimental evaluation is aimed to evaluate the practical
 267 applicability of the approach. We establish this by assessing the scalability of the approach on very
 268 large NNs and its practical reliability. As we discuss below, our findings suggest that the method
 269 scales to models such as vision transformers and video models that could not be verified before, and
 270 the implementation achieves the highest level of correctly answered verification queries.

271 In terms of geometric perturbations, we denote $R(\gamma)$ as the rotation operation, where the angle varies
 272 within the range $\pm\gamma$, and $S(\lambda)$ as the scaling operation, where the scaling factor ranges between $1 \pm \lambda$.
 273 Let $T(t)$ represent the translation operation, shifting an input by up to $\pm t$ proportionally in both the
 274 horizontal and vertical directions. Here we consider the combination of these three types of geometric
 275 transformations to evaluate the model’s robustness, both in terms of its adversarial accuracy, and its
 276 certified accuracy. The first measures the percentage of test inputs for which a counter-example was
 277 not found by the method. The second measures the percentage of samples reported to be robust in the
 278 geometric neighbourhood considered. Whenever a method can solve all queries the two measures
 279 are identical. We report only the highlights in the rest of this section but base our conclusions on the
 280 comprehensive benchmarking for the method also reported in the Appendix.

281 **Large NNs for Image Classification.** To evaluate the performance of HOVER on image classification
 282 for large NNs, we benchmarked the adversarial accuracy and certified accuracy obtained by the
 283 tool on 9 Models of different sizes, ranging from 19M (Gmlp) to 300M (Large Vit_{16×16}) tuneable
 284 parameters including several ResNet models, up to ResNet152, normally trained to a good level
 285 of accuracy. The dataset used is ImageNet on inputs of $3 \times 224 \times 224$. The verification queries
 286 consisted of any input transformation with rotation, translation and scaling with large parameters
 287 (20° , 10%, and 10%, respectively). To our knowledge, GeoRobust [22] is the only available tool that
 288 can handle such queries on high dimensional inputs for such large NNs. In particular, none of the
 289 tools in VNN-COMP [4], nor [21] can resolve such queries.

290 Table 1 reports the results obtained. From the results we find that HOVER significantly outperforms
 291 GeoRobust both in terms of adversarial and certified accuracy, and with a smaller number of undecided
 292 cases. GeoRobust is only shown to have superior performance on Large Vit_{16×16}, Gmlp and Swin.
 293 However, further analysis of these results indicate that GeoRobust often incorrectly concludes safety.
 294 Indeed, HOVER identified several counterexamples (6 for ResNet101, 7 for ResNet152, 18 for
 295 Swin) to verification queries that were reported *robust* by GeoRobust. We suspect this is because,
 296 without a sufficient number of iterations, GeoRobust’s underlying global optimisation can often use
 297 underestimations of the Lipschitz constant; this is a behaviour not discussed in [22].

298 The robustness results suggest that the ViT model is less robust than some ResNet models. This
 299 raises the question of why the patch-based attention mechanisms do not translate into improved
 300 robustness [26]. The results here only refer to geometric robustness and require further analysis.

301 **Large NNs for Video Classification.** To further evaluate the performance of HOVER we here
 302 report the results of the experiments that were ran to assess the robustness of large models used
 303 for video classification. For this we considered end-to-end RGB 3D-NNs without flow information
 304 trained on the Kinetics-400 dataset [27]. Specifically, we evaluated 6 pre-trained NNs from the
 305 open-source library PyTorchVideo [28], with network parameters ranging from 3.79M to 32.45M,
 306 and up to $32 \times 3 \times 256 \times 256$ input dimensions: Slow-R50 [29], R(2+1)D-R50 [30], X3D_M [31],
 307 I3D-R50 [32], CSN-R101 [33], and C2D-R50 [34].

308 For the evaluation, we randomly selected 200
 309 videos from the dataset and evaluated the ro-
 310 bustness of the models against perturbations
 311 applied to entire clips and single frames (see
 312 the Appendix for technical details). The pertur-
 313 bations consisted of combinations of rotation,
 314 scaling and translation, using the same pertur-
 315 bation intensity used for the images above.

316 To the best of our best knowledge, the only two
 317 verification methods applicable to video tasks
 318 are [35] and [36]. However, the methods can
 319 only scale to small NNs, hence they are not comparable to HOVER’s capabilities.

320 The results are reported in Table 2. It can be
 321 observed that HOVER was able to resolve a
 322 large proportion of the verification queries with
 323 a minimum rate of undecided cases. To our
 324 knowledge, this is the first time that large video
 325 classifiers are evaluated for local robustness.
 326 The results point to CSN-R101 and R(2+1)D-
 327 R50, which achieved the highest adversarial
 328 accuracy (47.0% and 45.0%) and certified accu-
 329 racy (44.0% and 45.0%). These findings indi-
 330 cate that architectural refinements and expanding
 331 model capacity could potentially benefit
 332 robustness against geometric transformations.

333 **Soundness Validation.** We discussed in Sec-
 334 tions 1 and 3 that the proposed verification
 335 method based on global optimisation may re-
 336 turn unsound results. As discussed, this the-
 337 oretical possibility may be mitigated, as it is
 338 routinely done in optimisation, by careful the
 339 choice of the optimisation parameters.

340 In what follows we evaluate the empirical
 341 soundness of HOVER. We do this in two ways.
 342 Firstly, we evaluate the results obtained by the
 343 tool on SoundnessBench [6]. This is a recently
 344 released neural network verification benchmark,
 345 which was designed for validating the correct-
 346 ness of verifiers by including the ground truth
 347 of the verification queries. Secondly, we re-
 348 port the results obtained by the tool against
 349 low-dimensionality perturbations from VNN-
 350 COMP [4]. In this case the ground truth is not
 351 known, but like VNN-COMP, we compare the results against those produced by SoA tools, by taking
 352 the agreement among all verifiers as ground truths. In total, we evaluate the soundness of HOVER
 353 about 500 results. All results produced by HOVER on SoundnessBench were correct (in line with
 354 the ground truth); all results produced by HOVER on the VNN-COMP tests were in line with those
 355 reported by the $\alpha\beta$ -CROWN [37].

Table 2: Benchmarking static geometric robustness of video classification models against geometric transforms ($R(20^\circ) + S(10\%) + T(10\%)$).

Model	Frame Length	Frame Rate	Params (M)	Clean Acc (%)	Adversarial Acc (%)	Certified Acc (%)
X3D_M	16	5	3.79	78.0	37.0	36.0
CSN-R101	32	2	22.21	79.0	47.0	44.0
C2D-R50	8	8	24.33	73.5	39.0	37.5
I3D-R50	8	8	28.04	73.0	42.5	42.0
R(2+1)D-R50	16	5	28.11	76.0	45.0	45.0
Slow-R50	8	8	32.45	76.5	44.0	43.0

Table 3: Soundness validation on SoundnessBench. Baseline performances are adopted from [6].

Benchmark	Input Dim	Tool	Verified	Falsified	Unknown	Unsound
CNN1	25-75	$\alpha\beta$ -CROWN	18	0	58	0
		PyRAT	10	0	66	0
		HOVER	25	0	51	0
CNN2	25-75	$\alpha\beta$ -CROWN	13	0	61	0
		PyRAT	5	0	69	0
		HOVER	17	0	57	0
CNN3	25-75	$\alpha\beta$ -CROWN	7	1	68	0
		PyRAT	5	0	71	0
		HOVER	11	0	65	0
CNN AvgPool	25-75	$\alpha\beta$ -CROWN	30	7	13	10
		PyRAT	0	0	60	0
		HOVER	16	0	44	0
CNN Tanh	25-75	$\alpha\beta$ -CROWN	0	0	38	0
		PyRAT	0	0	38	0
		HOVER	20	0	18	0
CNN Sigmoid	25-75	$\alpha\beta$ -CROWN	2	0	29	0
		PyRAT	2	0	29	0
		HOVER	19	2	10	0
MLP	10	$\alpha\beta$ -CROWN	20	2	49	0
		PyRAT	12	0	59	0
		HOVER	26	1	44	0

Table 4: Evaluation on two VNN-COMP benchmarks. Baseline performances are adopted from [4].

Benchmark	#Params	Tool	Verified	Falsified	Unknown	Unsound
CCTSDB Yolo	100K	$\alpha\beta$ -CROWN	11	28	0	0
		PyRAT	0	2	37	0
		HOVER	11	28	0	0
TLL Verify Bench	17k-67M	$\alpha\beta$ -CROWN	15	17	0	0
		PyRAT	15	17	0	0
		NeuralSAT	15	0	0	17
		HOVER	15	17	0	0

356 We report the results obtained on SoundnessBench on Table 3. The benchmark comprises 24 models
357 (primarily CNNs and MLPs) and includes 240 verification queries that ought to be resolved as
358 *robust* and 186 that ought to be resolved as *non-robust*. Note that the latter include carefully hidden
359 adversarial examples that are challenging for verifiers to discover. The performance of two SoA
360 verifiers, $\alpha\beta$ -CROWN [37] and pyRAT [38], are also reported for comparison. As shown, HOVER
361 returned the correct result for all the queries. Differently, $\alpha\beta$ -CROWN, which is regarded as SoA,
362 reported several incorrect results. We refer to the Appendix for detailed performance of each method.
363 Table 4 reports the results obtained on the CCTSDB Yolo and TLL Verify Bench benchmarks
364 from VNN-COMP [4]. The benchmarks were selected because of the low-input dimensionality
365 ($N = 2$) of the perturbations they consider, thus falling within the scope of HOVER. We observe
366 that HOVER achieves the same performance as $\alpha\beta$ -CROWN, without exhibiting any unknown or
367 unsound cases. Differently, another two SoA verifiers, PyRAT [38] and NeuralSAT [39], either fail to
368 prove robustness for several cases or report incorrect results.

369 5 Related work

370 An extensive body of literature exists on the verification of NNs against ℓ_p -bounded and other
371 perturbations; we refer to [2, 40] for a survey on the area. A variety of methods are used, from
372 Mixed-Integer Linear Programming [41–43], to SMT [39, 44], branch-and-bound [45–48], abstract
373 interpretation [38, 49–51], symbolic interval propagation methods [52–54]. Some of these methods,
374 notably symbolic interval propagation, outperform the present approach for large dimensionality
375 problems. However, as shown in the previous section, HOVER considerably outperforms all SoA on
376 geometric perturbations, including the approaches targetting geometric robustness directly [21, 22, 55–
377 57] (see also a discussion in the Appendix). Unlike the approach here presented, many of the cited
378 methods are shown to be theoretically sound. Yet, in practice, their theoretical soundness often
379 translates to unsound implementations, *e.g.*, floating point approximations [5] may impact the
380 soundness of the bounds generated by symbolic interval propagation methods. In turn, this results in
381 errors in actual verification experiments as recently confirmed in [6]. In Section 4, we empirically
382 validated HOVER and found not a single error in actual verification experiments; in contrast, we
383 found that some of the SoA tools, while theoretically sound, answered some queries incorrectly.

384 Much closer to HOVER are existing methods based on global optimisation [18, 24, 58]. The key
385 difference between HOVER and these methods is that the former couples Hölder optimisation with a
386 dimensionality reduction technique, thereby scaling to larger models and to higher dimensions, as
387 we empirically demonstrated. We note that existing optimisaton methods provably converge only if
388 particular (reliability) parameters can be chosen. However, this choice is closely related to providing
389 an upper bound of the Lipschitz constant. This is normally intractable for large models, for which
390 only estimations of the constant can be used in practice, thereby potentially resulting in unsound
391 results, as we empirically observed. In contrast, no incorrect results were produced by HOVER
392 during our extensive validation (see previous section).

393 6 Conclusions

394 We presented HOVER, a novel method for the verification of geometric robustness of NNs based on
395 Hölder optimisation and dimensionality reduction. We demonstrated that HOVER outperforms SoA
396 methods on vision classification models up to millions of tuneable parameters and large inputs, and
397 also enables the verification of large video classifiers for the first time. This makes it possible, we
398 believe for the first time, to apply verification methods to the validation in safety critical applications
399 in vision. While we do not provide a constructive proof of convergence, we validated the soundness
400 empirically by assessing the results on hundreds of queries. We observed that a robustness analysis
401 concerns the aggregation of several results and it is therefore not skewed by a very low error rate.
402 In terms of limitations of HOVER, the present SoA, notably symbolic interval propagation, scales
403 better on large dimensionality problems such as noise perturbations; so they remain the approach of
404 choice for those problems. In further work, we intend to focus on implementing HOVER in other
405 problems with low dimensionality such as contrast, luminosity, bias field [59] and blur [60] as well
406 as on extending the dimensionality reduction here devised to scale to more dimensions.

407 **References**

- 408 [1] Ian J Goodfellow, Jonathon Shlens, and Christian Szegedy. Explaining and harnessing adversarial examples. *arXiv preprint arXiv:1412.6572*, 2014.
- 410 [2] Xiaowei Huang, Daniel Kroening, Wenjie Ruan, James Sharp, Youcheng Sun, Emese Thamo, Min Wu, and Xinping Yi. A survey of safety and trustworthiness of deep neural networks: Verification, testing, adversarial attack and defence, and interpretability. *Computer Science Review*, 37:100270, 2020.
- 414 [3] Guy Katz, Clark Barrett, David L Dill, Kyle Julian, and Mykel J Kochenderfer. Reluplex: An efficient smt solver for verifying deep neural networks. In *Computer Aided Verification: 29th International Conference, CAV 2017, Heidelberg, Germany, July 24-28, 2017, Proceedings, Part I 30*, pages 97–117. Springer, 2017.
- 418 [4] Christopher Brix, Stanley Bak, Taylor T Johnson, and Haoze Wu. The fifth international verification of neural networks competition (vnn-comp 2024): Summary and results. *arXiv preprint arXiv:2412.19985*, 2024.
- 421 [5] Kai Jia and Martin Rinard. Exploiting verified neural networks via floating point numerical error. In *Static Analysis: 28th International Symposium, SAS 2021, Chicago, IL, USA, October 17–19, 2021, Proceedings 28*, pages 191–205. Springer, 2021.
- 424 [6] Xingjian Zhou, Hongji Xu, Andy Xu, Zhouxing Shi, Cho-Jui Hsieh, and Huan Zhang. Testing neural network verifiers: A soundness benchmark with hidden counterexamples. *arXiv preprint arXiv:2412.03154*, 2024.
- 427 [7] Naveed Akhtar, Ajmal Mian, Navid Kardan, and Mubarak Shah. Advances in adversarial attacks and defenses in computer vision: A survey. *IEEE Access*, 9:155161–155196, 2021.
- 430 [8] Alex Serban, Erik Poll, and Joost Visser. Adversarial examples on object recognition: A comprehensive survey. *ACM Computing Surveys (CSUR)*, 53(3):1–38, 2020.
- 433 [9] Daniela Lera and Ya D Sergeyev. Global minimization algorithms for holder functions. *BIT Numerical mathematics*, 42:119–133, 2002.
- 436 [10] Daniela Lera and Ya D Sergeyev. Lipschitz and hölder global optimization using space-filling curves. *Applied Numerical Mathematics*, 60(1-2):115–129, 2010.
- 439 [11] Yaroslav D Sergeyev, Roman G Strongin, and Daniela Lera. *Introduction to global optimization exploiting space-filling curves*. Springer Science & Business Media, 2013.
- 442 [12] Vladimir Grishagin, Ruslan Israfilov, and Yaroslav Sergeyev. Convergence conditions and numerical comparison of global optimization methods based on dimensionality reduction schemes. *Applied Mathematics and Computation*, 318:270–280, 2018.
- 445 [13] Houshang H Sohrab. *Basic real analysis*, volume 231. Springer, 2003.
- 448 [14] G Peano. Sur une courde qui remplit touteune aire plane. *Math. Ann.*, 36, 1890.
- 451 [15] David Hubert. Ueber die stetige abbildung einer linie auf ein flächenstück. *Mathematische Annalen*, 38:459–460, 1891.
- 454 [16] Roman G Strongin and Yaroslav D Sergeyev. *Global optimization with non-convex constraints: Sequential and parallel algorithms*, volume 45. Springer Science & Business Media, 2013.
- 457 [17] C Szegedy. Intriguing properties of neural networks. *arXiv preprint arXiv:1312.6199*, 2013.
- 460 [18] Wenjie Ruan, Xiaowei Huang, and Marta Kwiatkowska. Reachability analysis of deep neural networks with provable guarantees. In *Proceedings of the 27th International Joint Conference on Artificial Intelligence*, pages 2651–2659, 2018.
- 463 [19] Panagiotis Kouvaros and Alessio Lomuscio. Formal verification of cnn-based perception systems. *arXiv preprint arXiv:1811.11373*, 2018.

- 452 [20] Max Jaderberg, Karen Simonyan, Andrew Zisserman, et al. Spatial transformer networks.
 453 *Advances in neural information processing systems*, 2015.
- 454 [21] Ben Batten, Yang Zheng, Alessandro De Palma, Panagiotis Kouvaros, and Alessio Lomuscio.
 455 Verification of geometric robustness of neural networks via piecewise linear approximation and
 456 lipschitz optimisation. In *ECAI 2024*, pages 2362–2369. IOS Press, 2024.
- 457 [22] Fu Wang, Peipei Xu, Wenjie Ruan, and Xiaowei Huang. Towards verifying the geometric
 458 robustness of large-scale neural networks. In *Proceedings of the AAAI Conference on Artificial
 459 Intelligence*, volume 37, pages 15197–15205, 2023.
- 460 [23] Eric Gourdin, Brigitte Jaumard, and Rachid Ellaia. Global optimization of hölder functions.
 461 *Journal of Global Optimization*, 8:323–348, 1996.
- 462 [24] Chi Zhang, Zhen Chen, Peipei Xu, Geyong Min, and Wenjie Ruan. Verification on out-of-
 463 distribution detectors under natural perturbations. *Machine Learning*, 114(3):77, 2025.
- 464 [25] Gabriel Altay. Hilbertcurve.
- 465 [26] Daquan Zhou, Zhiding Yu, Enze Xie, Chaowei Xiao, Animashree Anandkumar, Jiashi Feng,
 466 and Jose M Alvarez. Understanding the robustness in vision transformers. In *International
 467 conference on machine learning*, pages 27378–27394. PMLR, 2022.
- 468 [27] Will Kay, Joao Carreira, Karen Simonyan, Brian Zhang, Chloe Hillier, Sudheendra Vijaya-
 469 narasimhan, Fabio Viola, Tim Green, Trevor Back, Paul Natsev, et al. The kinetics human
 470 action video dataset. *arXiv preprint arXiv:1705.06950*, 2017.
- 471 [28] Haoqi Fan, Tullie Murrell, Heng Wang, Kalyan Vasudev Alwala, Yanghao Li, Yilei Li, Bo Xiong,
 472 Nikhila Ravi, Meng Li, Haichuan Yang, et al. Pytorchvideo: A deep learning library for video
 473 understanding. In *Proceedings of the 29th ACM international conference on multimedia*, pages
 474 3783–3786, 2021.
- 475 [29] Kensho Hara, Hirokatsu Kataoka, and Yutaka Satoh. Learning spatio-temporal features with 3d
 476 residual networks for action recognition. In *Proceedings of the IEEE international conference
 477 on computer vision workshops*, pages 3154–3160, 2017.
- 478 [30] Du Tran, Heng Wang, Lorenzo Torresani, Jamie Ray, Yann LeCun, and Manohar Paluri. A
 479 closer look at spatiotemporal convolutions for action recognition. In *Proceedings of the IEEE
 480 conference on Computer Vision and Pattern Recognition*, pages 6450–6459, 2018.
- 481 [31] Christoph Feichtenhofer. X3d: Expanding architectures for efficient video recognition. In
 482 *Proceedings of the IEEE/CVF conference on computer vision and pattern recognition*, pages
 483 203–213, 2020.
- 484 [32] Joao Carreira and Andrew Zisserman. Quo vadis, action recognition? a new model and the
 485 kinetics dataset. In *proceedings of the IEEE Conference on Computer Vision and Pattern
 486 Recognition*, pages 6299–6308, 2017.
- 487 [33] Du Tran, Heng Wang, Lorenzo Torresani, and Matt Feiszli. Video classification with channel-
 488 separated convolutional networks. In *Proceedings of the IEEE/CVF international conference
 489 on computer vision*, pages 5552–5561, 2019.
- 490 [34] Xiaolong Wang, Ross Girshick, Abhinav Gupta, and Kaiming He. Non-local neural networks.
 491 In *Proceedings of the IEEE conference on computer vision and pattern recognition*, pages
 492 7794–7803, 2018.
- 493 [35] Min Wu and Marta Kwiatkowska. Robustness guarantees for deep neural networks on videos.
 494 In *Proceedings of the IEEE/CVF Conference on Computer Vision and Pattern Recognition*,
 495 pages 311–320, 2020.
- 496 [36] Samuel Sasaki, Diego Manzanas Lopez, Preston K Robinette, and Taylor T Johnson. Robustness
 497 verification of video classification neural networks.

- 498 [37] Huan Zhang, Shiqi Wang, Kaidi Xu, Linyi Li, Bo Li, Suman Jana, Cho-Jui Hsieh, and J Zico
 499 Kolter. General cutting planes for bound-propagation-based neural network verification. *Advances in neural information processing systems*, 35:1656–1670, 2022.
- 500
- 501 [38] Augustin Lemesele, Julien Lehmann, and Tristan Le Gall. Neural network verification with pyrat.
 502 *arXiv preprint arXiv:2410.23903*, 2024.
- 503 [39] Hai Duong, ThanhVu Nguyen, and Matthew Dwyer. A dpll (t) framework for verifying deep
 504 neural networks. *arXiv preprint arXiv:2307.10266*, 2023.
- 505 [40] Changliu Liu, Tomer Arnon, Christopher Lazarus, Christopher Strong, Clark Barrett, Mykel J
 506 Kochenderfer, et al. Algorithms for verifying deep neural networks. *Foundations and Trends®*
 507 in *Optimization*, 4(3-4):244–404, 2021.
- 508 [41] Vincent Tjeng, Kai Xiao, and Russ Tedrake. Evaluating robustness of neural networks with
 509 mixed integer programming. *arXiv preprint arXiv:1711.07356*, 2017.
- 510 [42] Alessio Lomuscio and Lalit Maganti. An approach to reachability analysis for feed-forward
 511 relu neural networks. *arXiv preprint arXiv:1706.07351*, 2017.
- 512 [43] Panagiotis Kouvaros and Alessio Lomuscio. Towards scalable complete verification of relu
 513 neural networks via dependency-based branching. In *IJCAI*, pages 2643–2650, 2021.
- 514 [44] Haoze Wu, Omri Isac, Aleksandar Zeljić, Teruhiro Tagomori, Matthew Daggitt, Wen Kokke,
 515 Idan Refaeli, Guy Amir, Kyle Julian, Shahaf Bassan, et al. Marabou 2.0: a versatile formal
 516 analyzer of neural networks. In *International Conference on Computer Aided Verification*, pages
 517 249–264. Springer, 2024.
- 518 [45] Kaidi Xu, Huan Zhang, Shiqi Wang, Yihan Wang, Suman Jana, Xue Lin, and Cho-Jui Hsieh.
 519 Fast and complete: Enabling complete neural network verification with rapid and massively
 520 parallel incomplete verifiers. In *International Conference on Learning Representations*, 2021.
- 521 [46] Rudy Bunel, Jingyue Lu, Ilker Turkaslan, Philip HS Torr, Pushmeet Kohli, and M Pawan
 522 Kumar. Branch and bound for piecewise linear neural network verification. *Journal of Machine
 523 Learning Research*, 21(42):1–39, 2020.
- 524 [47] Huan Zhang, Tsui-Wei Weng, Pin-Yu Chen, Cho-Jui Hsieh, and Luca Daniel. Efficient neu-
 525 ral network robustness certification with general activation functions. *Advances in neural
 526 information processing systems*, 31, 2018.
- 527 [48] Shiqi Wang, Huan Zhang, Kaidi Xu, Xue Lin, Suman Jana, Cho-Jui Hsieh, and J Zico Kolter.
 528 Beta-crown: Efficient bound propagation with per-neuron split constraints for neural network
 529 robustness verification. *Advances in Neural Information Processing Systems*, 34:29909–29921,
 530 2021.
- 531 [49] Timon Gehr, Matthew Mirman, Dana Drachsler-Cohen, Petar Tsankov, Swarat Chaudhuri,
 532 and Martin Vechev. Ai2: Safety and robustness certification of neural networks with abstract
 533 interpretation. In *2018 IEEE symposium on security and privacy (SP)*, pages 3–18. IEEE, 2018.
- 534 [50] Gagandeep Singh, Timon Gehr, Matthew Mirman, Markus Püschel, and Martin Vechev. Fast
 535 and effective robustness certification. *Advances in neural information processing systems*, 31,
 536 2018.
- 537 [51] Gagandeep Singh, Timon Gehr, Markus Püschel, and Martin Vechev. An abstract domain for
 538 certifying neural networks. *Proceedings of the ACM on Programming Languages*, 3(POPL):1–
 539 30, 2019.
- 540 [52] Elena Botoeva, Panagiotis Kouvaros, Jan Kronqvist, Alessio Lomuscio, and Ruth Misener.
 541 Efficient verification of relu-based neural networks via dependency analysis. In *Proceedings of
 542 the AAAI Conference on Artificial Intelligence*, volume 34, pages 3291–3299, 2020.
- 543 [53] Patrick Henriksen and Alessio Lomuscio. Deepsplit: An efficient splitting method for neural
 544 network verification via indirect effect analysis. In *IJCAI*, pages 2549–2555, 2021.

- 545 [54] Panagiotis Kouvaros, Benedikt Brückner, Patrick Henriksen, and Alessio Lomuscio. Dynamic
546 back-substitution in bound-propagation-based neural network verification. In *Proceedings of*
547 *the AAAI Conference on Artificial Intelligence*, volume 39, pages 27383–27391, 2025.
- 548 [55] Linyi Li, Maurice Weber, Xiaojun Xu, Luka Rimanic, Bhavya Kailkhura, Tao Xie, Ce Zhang,
549 and Bo Li. Tss: Transformation-specific smoothing for robustness certification. In *Proceedings*
550 *of the 2021 ACM SIGSAC Conference on Computer and Communications Security*, pages
551 535–557, 2021.
- 552 [56] Zhongkai Hao, Chengyang Ying, Yinpeng Dong, Hang Su, Jian Song, and Jun Zhu. Gsmooth:
553 Certified robustness against semantic transformations via generalized randomized smoothing.
554 In *International Conference on Machine Learning*, pages 8465–8483. PMLR, 2022.
- 555 [57] Mislav Balunovic, Maximilian Baader, Gagandeep Singh, Timon Gehr, and Martin Vechev.
556 Certifying geometric robustness of neural networks. *Advances in Neural Information Processing*
557 *Systems*, 32, 2019.
- 558 [58] Chi Zhang, Wenjie Ruan, and Peipei Xu. Reachability analysis of neural network control
559 systems. In *Proceedings of the AAAI Conference on Artificial Intelligence*, volume 37, pages
560 15287–15295, 2023.
- 561 [59] Patrick Henriksen and Alessio Lomuscio. Robust training of neural networks against bias field
562 perturbations. In *Proceedings of the AAAI Conference on Artificial Intelligence*, volume 37,
563 pages 14865–14873, 2023.
- 564 [60] Benedikt Brückner and Alessio Lomuscio. Verification of neural networks against convolutional
565 perturbations via parameterised kernels. In *Proceedings of the AAAI Conference on Artificial*
566 *Intelligence*, volume 39, pages 27215–27223, 2025.

567 **NeurIPS Paper Checklist**

568 **1. Claims**

569 Question: Do the main claims made in the abstract and introduction accurately reflect the
570 paper's contributions and scope?

571 Answer: [Yes]

572 Justification: The abstract and introduction have clearly stated the main contributions, scope
573 and potential limitation.

574 Guidelines:

- 575 • The answer NA means that the abstract and introduction do not include the claims
576 made in the paper.
- 577 • The abstract and/or introduction should clearly state the claims made, including the
578 contributions made in the paper and important assumptions and limitations. A No or
579 NA answer to this question will not be perceived well by the reviewers.
- 580 • The claims made should match theoretical and experimental results, and reflect how
581 much the results can be expected to generalize to other settings.
- 582 • It is fine to include aspirational goals as motivation as long as it is clear that these goals
583 are not attained by the paper.

584 **2. Limitations**

585 Question: Does the paper discuss the limitations of the work performed by the authors?

586 Answer: [Yes]

587 Justification: We discuss the limitation and potentially unsound results may be obtained via
588 our algorithm, but this seldom happens.

589 Guidelines:

- 590 • The answer NA means that the paper has no limitation while the answer No means that
591 the paper has limitations, but those are not discussed in the paper.
- 592 • The authors are encouraged to create a separate "Limitations" section in their paper.
- 593 • The paper should point out any strong assumptions and how robust the results are to
594 violations of these assumptions (e.g., independence assumptions, noiseless settings,
595 model well-specification, asymptotic approximations only holding locally). The authors
596 should reflect on how these assumptions might be violated in practice and what the
597 implications would be.
- 598 • The authors should reflect on the scope of the claims made, e.g., if the approach was
599 only tested on a few datasets or with a few runs. In general, empirical results often
600 depend on implicit assumptions, which should be articulated.
- 601 • The authors should reflect on the factors that influence the performance of the approach.
602 For example, a facial recognition algorithm may perform poorly when image resolution
603 is low or images are taken in low lighting. Or a speech-to-text system might not be
604 used reliably to provide closed captions for online lectures because it fails to handle
605 technical jargon.
- 606 • The authors should discuss the computational efficiency of the proposed algorithms
607 and how they scale with dataset size.
- 608 • If applicable, the authors should discuss possible limitations of their approach to
609 address problems of privacy and fairness.
- 610 • While the authors might fear that complete honesty about limitations might be used by
611 reviewers as grounds for rejection, a worse outcome might be that reviewers discover
612 limitations that aren't acknowledged in the paper. The authors should use their best
613 judgment and recognize that individual actions in favor of transparency play an impor-
614 tant role in developing norms that preserve the integrity of the community. Reviewers
615 will be specifically instructed to not penalize honesty concerning limitations.

616 **3. Theory assumptions and proofs**

617 Question: For each theoretical result, does the paper provide the full set of assumptions and
618 a complete (and correct) proof?

619 Answer: [Yes]

620 Justification: The complete proofs are provided in the appendix. Theorems are properly
621 referenced in this paper.

622 Guidelines:

- 623 • The answer NA means that the paper does not include theoretical results.
- 624 • All the theorems, formulas, and proofs in the paper should be numbered and cross-
625 referenced.
- 626 • All assumptions should be clearly stated or referenced in the statement of any theorems.
- 627 • The proofs can either appear in the main paper or the supplemental material, but if
628 they appear in the supplemental material, the authors are encouraged to provide a short
629 proof sketch to provide intuition.
- 630 • Inversely, any informal proof provided in the core of the paper should be complemented
631 by formal proofs provided in appendix or supplemental material.
- 632 • Theorems and Lemmas that the proof relies upon should be properly referenced.

633 **4. Experimental result reproducibility**

634 Question: Does the paper fully disclose all the information needed to reproduce the main ex-
635 perimental results of the paper to the extent that it affects the main claims and/or conclusions
636 of the paper (regardless of whether the code and data are provided or not)?

637 Answer: [Yes]

638 Justification: We describe the proposed algorithm in detail and include its pseudocode in
639 the Appendix. An experienced researcher should be able to reproduce the method within a
640 reasonable time. The code will be open-sourced.

641 Guidelines:

- 642 • The answer NA means that the paper does not include experiments.
- 643 • If the paper includes experiments, a No answer to this question will not be perceived
644 well by the reviewers: Making the paper reproducible is important, regardless of
645 whether the code and data are provided or not.
- 646 • If the contribution is a dataset and/or model, the authors should describe the steps taken
647 to make their results reproducible or verifiable.
- 648 • Depending on the contribution, reproducibility can be accomplished in various ways.
649 For example, if the contribution is a novel architecture, describing the architecture fully
650 might suffice, or if the contribution is a specific model and empirical evaluation, it may
651 be necessary to either make it possible for others to replicate the model with the same
652 dataset, or provide access to the model. In general, releasing code and data is often
653 one good way to accomplish this, but reproducibility can also be provided via detailed
654 instructions for how to replicate the results, access to a hosted model (e.g., in the case
655 of a large language model), releasing of a model checkpoint, or other means that are
656 appropriate to the research performed.
- 657 • While NeurIPS does not require releasing code, the conference does require all submis-
658 sions to provide some reasonable avenue for reproducibility, which may depend on the
659 nature of the contribution. For example
 - 660 (a) If the contribution is primarily a new algorithm, the paper should make it clear how
661 to reproduce that algorithm.
 - 662 (b) If the contribution is primarily a new model architecture, the paper should describe
663 the architecture clearly and fully.
 - 664 (c) If the contribution is a new model (e.g., a large language model), then there should
665 either be a way to access this model for reproducing the results or a way to reproduce
666 the model (e.g., with an open-source dataset or instructions for how to construct
667 the dataset).
 - 668 (d) We recognize that reproducibility may be tricky in some cases, in which case
669 authors are welcome to describe the particular way they provide for reproducibility.
670 In the case of closed-source models, it may be that access to the model is limited in
671 some way (e.g., to registered users), but it should be possible for other researchers
672 to have some path to reproducing or verifying the results.

673 **5. Open access to data and code**

674 Question: Does the paper provide open access to the data and code, with sufficient instruc-
675 tions to faithfully reproduce the main experimental results, as described in supplemental
676 material?

677 Answer: [No]

678 Justification: The code will be open-sourced, and the datasets we evaluate are publicly
679 available; no private benchmarks are used.

680 Guidelines:

- 681 • The answer NA means that paper does not include experiments requiring code.
- 682 • Please see the NeurIPS code and data submission guidelines (<https://nips.cc/public/guides/CodeSubmissionPolicy>) for more details.
- 684 • While we encourage the release of code and data, we understand that this might not be
685 possible, so “No” is an acceptable answer. Papers cannot be rejected simply for not
686 including code, unless this is central to the contribution (e.g., for a new open-source
687 benchmark).
- 688 • The instructions should contain the exact command and environment needed to run to
689 reproduce the results. See the NeurIPS code and data submission guidelines (<https://nips.cc/public/guides/CodeSubmissionPolicy>) for more details.
- 691 • The authors should provide instructions on data access and preparation, including how
692 to access the raw data, preprocessed data, intermediate data, and generated data, etc.
- 693 • The authors should provide scripts to reproduce all experimental results for the new
694 proposed method and baselines. If only a subset of experiments are reproducible, they
695 should state which ones are omitted from the script and why.
- 696 • At submission time, to preserve anonymity, the authors should release anonymized
697 versions (if applicable).
- 698 • Providing as much information as possible in supplemental material (appended to the
699 paper) is recommended, but including URLs to data and code is permitted.

700 **6. Experimental setting/details**

701 Question: Does the paper specify all the training and test details (e.g., data splits, hyper-
702 parameters, how they were chosen, type of optimizer, etc.) necessary to understand the
703 results?

704 Answer: [Yes]

705 Justification: Detailed settings for our experiments are provided in the experiments section
706 and in the Appendix.

707 Guidelines:

- 708 • The answer NA means that the paper does not include experiments.
- 709 • The experimental setting should be presented in the core of the paper to a level of detail
710 that is necessary to appreciate the results and make sense of them.
- 711 • The full details can be provided either with the code, in appendix, or as supplemental
712 material.

713 **7. Experiment statistical significance**

714 Question: Does the paper report error bars suitably and correctly defined or other appropriate
715 information about the statistical significance of the experiments?

716 Answer: [Yes]

717 Justification: Our method is deterministic, producing identical results when executed on the
718 same machine.

719 Guidelines:

- 720 • The answer NA means that the paper does not include experiments.
- 721 • The authors should answer "Yes" if the results are accompanied by error bars, confi-
722 dence intervals, or statistical significance tests, at least for the experiments that support
723 the main claims of the paper.

- 724 • The factors of variability that the error bars are capturing should be clearly stated (for
 725 example, train/test split, initialization, random drawing of some parameter, or overall
 726 run with given experimental conditions).
 727 • The method for calculating the error bars should be explained (closed form formula,
 728 call to a library function, bootstrap, etc.)
 729 • The assumptions made should be given (e.g., Normally distributed errors).
 730 • It should be clear whether the error bar is the standard deviation or the standard error
 731 of the mean.
 732 • It is OK to report 1-sigma error bars, but one should state it. The authors should
 733 preferably report a 2-sigma error bar than state that they have a 96% CI, if the hypothesis
 734 of Normality of errors is not verified.
 735 • For asymmetric distributions, the authors should be careful not to show in tables or
 736 figures symmetric error bars that would yield results that are out of range (e.g. negative
 737 error rates).
 738 • If error bars are reported in tables or plots, The authors should explain in the text how
 739 they were calculated and reference the corresponding figures or tables in the text.

740 **8. Experiments compute resources**

741 Question: For each experiment, does the paper provide sufficient information on the com-
 742 puter resources (type of compute workers, memory, time of execution) needed to reproduce
 743 the experiments?

744 Answer: [Yes]

745 Justification: Detailed settings, environment configurations, and software package informa-
 746 tion for our experiments are provided in the experiments section and in the Appendix.

747 Guidelines:

- 748 • The answer NA means that the paper does not include experiments.
 749 • The paper should indicate the type of compute workers CPU or GPU, internal cluster,
 750 or cloud provider, including relevant memory and storage.
 751 • The paper should provide the amount of compute required for each of the individual
 752 experimental runs as well as estimate the total compute.
 753 • The paper should disclose whether the full research project required more compute
 754 than the experiments reported in the paper (e.g., preliminary or failed experiments that
 755 didn't make it into the paper).

756 **9. Code of ethics**

757 Question: Does the research conducted in the paper conform, in every respect, with the
 758 NeurIPS Code of Ethics <https://neurips.cc/public/EthicsGuidelines>?

759 Answer: [Yes]

760 Justification: We have read and acknowledged the NeurIPS Code of Ethics.

761 Guidelines:

- 762 • The answer NA means that the authors have not reviewed the NeurIPS Code of Ethics.
 763 • If the authors answer No, they should explain the special circumstances that require a
 764 deviation from the Code of Ethics.
 765 • The authors should make sure to preserve anonymity (e.g., if there is a special consid-
 766 eration due to laws or regulations in their jurisdiction).

767 **10. Broader impacts**

768 Question: Does the paper discuss both potential positive societal impacts and negative
 769 societal impacts of the work performed?

770 Answer: [Yes]

771 Justification: Societal impacts have been discussed explicitly in the introduction. As the
 772 paper concerns a technical approach to AI Safety. Specifically, it is intended to contribute
 773 towards the assessment of AI systems before they are deployed. We regard this as a strongly
 774 positive social impact.

775 Guidelines:

- The answer NA means that there is no societal impact of the work performed.
- If the authors answer NA or No, they should explain why their work has no societal impact or why the paper does not address societal impact.
- Examples of negative societal impacts include potential malicious or unintended uses (e.g., disinformation, generating fake profiles, surveillance), fairness considerations (e.g., deployment of technologies that could make decisions that unfairly impact specific groups), privacy considerations, and security considerations.
- The conference expects that many papers will be foundational research and not tied to particular applications, let alone deployments. However, if there is a direct path to any negative applications, the authors should point it out. For example, it is legitimate to point out that an improvement in the quality of generative models could be used to generate deepfakes for disinformation. On the other hand, it is not needed to point out that a generic algorithm for optimizing neural networks could enable people to train models that generate Deepfakes faster.
- The authors should consider possible harms that could arise when the technology is being used as intended and functioning correctly, harms that could arise when the technology is being used as intended but gives incorrect results, and harms following from (intentional or unintentional) misuse of the technology.
- If there are negative societal impacts, the authors could also discuss possible mitigation strategies (e.g., gated release of models, providing defenses in addition to attacks, mechanisms for monitoring misuse, mechanisms to monitor how a system learns from feedback over time, improving the efficiency and accessibility of ML).

798 **11. Safeguards**

799 Question: Does the paper describe safeguards that have been put in place for responsible
800 release of data or models that have a high risk for misuse (e.g., pretrained language models,
801 image generators, or scraped datasets)?

802 Answer: [NA]

803 Justification: The paper poses no such risks.

804 Guidelines:

- The answer NA means that the paper poses no such risks.
- Released models that have a high risk for misuse or dual-use should be released with necessary safeguards to allow for controlled use of the model, for example by requiring that users adhere to usage guidelines or restrictions to access the model or implementing safety filters.
- Datasets that have been scraped from the Internet could pose safety risks. The authors should describe how they avoided releasing unsafe images.
- We recognize that providing effective safeguards is challenging, and many papers do not require this, but we encourage authors to take this into account and make a best faith effort.

815 **12. Licenses for existing assets**

816 Question: Are the creators or original owners of assets (e.g., code, data, models), used in
817 the paper, properly credited and are the license and terms of use explicitly mentioned and
818 properly respected?

819 Answer: [Yes]

820 Justification: We have properly cited the original paper that produced the code package or
821 dataset.

822 Guidelines:

- The answer NA means that the paper does not use existing assets.
- The authors should cite the original paper that produced the code package or dataset.
- The authors should state which version of the asset is used and, if possible, include a URL.
- The name of the license (e.g., CC-BY 4.0) should be included for each asset.

- 828 • For scraped data from a particular source (e.g., website), the copyright and terms of
829 service of that source should be provided.
830 • If assets are released, the license, copyright information, and terms of use in the
831 package should be provided. For popular datasets, paperswithcode.com/datasets
832 has curated licenses for some datasets. Their licensing guide can help determine the
833 license of a dataset.
834 • For existing datasets that are re-packaged, both the original license and the license of
835 the derived asset (if it has changed) should be provided.
836 • If this information is not available online, the authors are encouraged to reach out to
837 the asset's creators.

838 **13. New assets**

839 Question: Are new assets introduced in the paper well documented and is the documentation
840 provided alongside the assets?

841 Answer: [NA]

842 Justification: The paper does not release new assets.

843 Guidelines:

- 844 • The answer NA means that the paper does not release new assets.
845 • Researchers should communicate the details of the dataset/code/model as part of their
846 submissions via structured templates. This includes details about training, license,
847 limitations, etc.
848 • The paper should discuss whether and how consent was obtained from people whose
849 asset is used.
850 • At submission time, remember to anonymize your assets (if applicable). You can either
851 create an anonymized URL or include an anonymized zip file.

852 **14. Crowdsourcing and research with human subjects**

853 Question: For crowdsourcing experiments and research with human subjects, does the paper
854 include the full text of instructions given to participants and screenshots, if applicable, as
855 well as details about compensation (if any)?

856 Answer: [NA]

857 Justification: The paper does not involve crowdsourcing nor research with human subjects.

858 Guidelines:

- 859 • The answer NA means that the paper does not involve crowdsourcing nor research with
860 human subjects.
861 • Including this information in the supplemental material is fine, but if the main contribu-
862 tion of the paper involves human subjects, then as much detail as possible should be
863 included in the main paper.
864 • According to the NeurIPS Code of Ethics, workers involved in data collection, curation,
865 or other labor should be paid at least the minimum wage in the country of the data
866 collector.

867 **15. Institutional review board (IRB) approvals or equivalent for research with human
868 subjects**

869 Question: Does the paper describe potential risks incurred by study participants, whether
870 such risks were disclosed to the subjects, and whether Institutional Review Board (IRB)
871 approvals (or an equivalent approval/review based on the requirements of your country or
872 institution) were obtained?

873 Answer: [NA]

874 Justification: The paper does not involve crowdsourcing nor research with human subjects.

875 Guidelines:

- 876 • The answer NA means that the paper does not involve crowdsourcing nor research with
877 human subjects.

- 878 • Depending on the country in which research is conducted, IRB approval (or equivalent)
879 may be required for any human subjects research. If you obtained IRB approval, you
880 should clearly state this in the paper.
881 • We recognize that the procedures for this may vary significantly between institutions
882 and locations, and we expect authors to adhere to the NeurIPS Code of Ethics and the
883 guidelines for their institution.
884 • For initial submissions, do not include any information that would break anonymity (if
885 applicable), such as the institution conducting the review.

886 **16. Declaration of LLM usage**

887 Question: Does the paper describe the usage of LLMs if it is an important, original, or
888 non-standard component of the core methods in this research? Note that if the LLM is used
889 only for writing, editing, or formatting purposes and does not impact the core methodology,
890 scientific rigorousness, or originality of the research, declaration is not required.

891 Answer: [NA]

892 Justification: The core method development in this research does not involve LLMs as any
893 important, original, or non-standard components.

894 Guidelines:

- 895 • The answer NA means that the core method development in this research does not
896 involve LLMs as any important, original, or non-standard components.
897 • Please refer to our LLM policy (<https://neurips.cc/Conferences/2025/LLM>)
898 for what should or should not be described.